Application of *ab initio* Quantum-Chemical Cluster Calculations for the Study of Electronic Multiplet Structure of Transition Metal Ions and Their Exchange Interaction in Perovskites

L. Siurakshina

e-mail: siuraksh@jinr.ru, Laboratory of Information Technologies, JINR, Dubna

I. Soft X-ray resonant inelastic scattering (RIXS) is increasingly important in the study of electronic properties of strongly correlated $3d$ systems[1]. Measurements of d-d excitations that correspond to local rearrangements of the valence $3d$ electrons provide a valuable piece of information on the interplay between spin, orbital and lattice degrees of freedom in these systems.

Spectral properties related to the low-energy d-d excitations in nearly cubic vanadium perovskites RVO_3 (with R=Y or trivalent rare earth ion) have been examined by us[2] for the expected L-edge resonant inelastic X-ray scattering measurements. Multiplet structure of V^{3+} ion in the basic t_{2g}^2 electron configuration is calculated with the help of *ab initio* quantum-chemical(QC) method applied to $[R_8VO_6]^{15+}$ cluster, Fig.1, embedded in a crystalline environment. The relative energy position of different terms can be well described as follows:

$$\mathcal{E}(^3A_2) = \Delta_t,\ \mathcal{E}(^1A_1') = 2J_H - \Delta\mathcal{E}',\ \mathcal{E}(^1E) = 2J_H,$$
$$\mathcal{E}(^1B_1) = \mathcal{E}(^1B_2) = \Delta_t + 2J_H,\ \mathcal{E}(^1A_1) = 5J_H + \Delta\mathcal{E}',$$

where $\Delta\mathcal{E}' \approx \Delta_t[1 + (\Delta_t/J_H)]/3$, for $\Delta_t/J_H < 1/2$. For YVO_3, the QC calculations yield the estimates $\Delta_t \approx 0.2$eV and $J_H \approx 0.5$eV.

In our QC cluster approach[3] based on the use of MOLPRO computer program [4], the wavefunctions and energies of electron configurations are calculated at different levels of accuracy - from the Hartree-Fock self-consistent field (HFSCF) method through a multi-configuration self-consistent field (MCSCF) ansatz to the multi-reference configuration-interaction method (MRCI).

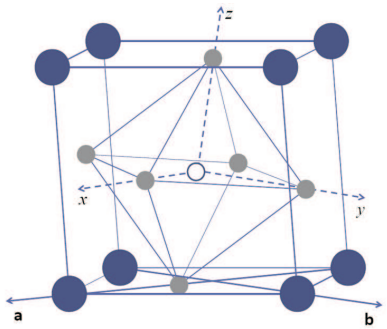

Figure 1: Cluster $[Y_8VO_6]^{15+}$ chosen for quantum chemical calculations. The large dark circles are yttrium, the smaller grey circles are oxygen, and the central open circle is vanadium.

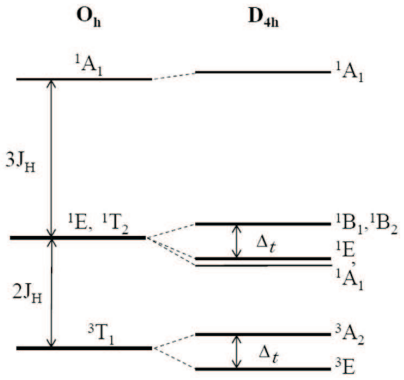

Figure 2: Multiplet structure of t_{2g}^2 configuration of V^{3+} ion in crystal field of D_{4h} symmetry. In RIXS the initial (ground) state is given by ^3E and other terms correspond to local $d-d$ excitations.

The term energies obtained in the MRCI calculations are given schematically in Fig.2. The low-energy part of the RIXS spectra is expected to exhibit the multiplet structure of t_{2g}^2 configuration.

RIXS is described by second-order processes of interaction between photons and a matter.The incoming photon with momentum $\hbar\mathbf{k}$ and energy $\hbar\omega_{\mathbf{k}}$ tuned close to the L-edge absorption promotes an electron from the $2p$ shell to an empty $3d$ valence state, thus producing an intermediate core-hole state $|(t_{2g}^3\underline{p})_{[i]}\rangle$. In a subsequent radiative decay of the core hole the emitted $(\hbar\mathbf{k}', \hbar\omega_{\mathbf{k}'})$ photon leaves the $3d$ electron system in an excited state $|(t_{2g}^2)_{[f]}\rangle$ with momentum $\hbar(\mathbf{k} - \mathbf{k}')$ and energy $\hbar(\omega_{\mathbf{k}} - \omega_{\mathbf{k}'})$ that are measured. For given polarization vectors $\boldsymbol{\epsilon}$ and $\boldsymbol{\epsilon}'$ of the incoming and and outgoing photons, respectively, the scattering amplitude of the second-order resonant processes governed by the transition dipole operator $\mathbf{D_k}$ can be written as [1]:

$$\mathcal{F}_{fg}^{\epsilon'\epsilon}(\mathbf{k}', \mathbf{k}; z_k) = \qquad (1)$$

$$\langle (t_{2g}^2)_{[f]}|(\boldsymbol{\epsilon}'\mathbf{D}_{\mathbf{k}'})^\dagger \mathcal{G}(z_{\mathbf{k}})(\boldsymbol{\epsilon}\mathbf{D}_{\mathbf{k}})|(t_{2g}^2)_{[g]}\rangle$$

Here, the initial (ground) and excited (final) states are denoted as $|(t_{2g}^2)_{[g]}\rangle$ and $|(t_{2g}^2)_{[f]}\rangle$, respectively, $[g]$ and $[f]$ are the shortenings for the quantum numbers. $\mathcal{G}(z_{\mathbf{k}})$ is the intermediate-state propagator which describes the system in the presence of a core hole:

$$\mathcal{G}(z_{\mathbf{k}}) = \sum_{\{i\}} \frac{|(t_{2g}^3\underline{p})_{[i]}\rangle\langle(t_{2g}^3\underline{p})_{[i]}|}{z_{\mathbf{k}} - E_{[i]}}, \qquad (2)$$

where $z_{\mathbf{k}} = \hbar\omega_{\mathbf{k}} + i\Upsilon$, for $E_{[g]} = 0$, and the lifetime broadening Υ of intermediate core-hole states is taken to be independent on the state index $[i]$.

In the intermediate states of the RIXS process the induced $2p$-core hole was taken into account by including strong $2p$-$3d$ electron interactions. A symmetry-group approach was applied to generate the basis set of many-electron wavefunctions of the intermediate core-hole states accessible in RIXS processes. Although a comprehensive description of the core-hole multiplets still remains a formidable task and requires using specially designed numerical codes, for particular resonant states the analysis was simplified and the calculation of RIXS amplitude have been carried out analytically to the end.[2]

II. In the work [5] we have implemented *ab initio* QC cluster calculations to the analysis of magnetic interactions in layered iridate Ba_2IrO_4. Peculiar magnetic properties of layered iridium oxides like A_2IrO_4 (A=Sr, Ba) and Na_2IrO_3 are due to delicate cooperation of electron hopping, on-site Coulomb and exchange interactions, crystal-field splitting of t_{2g} orbitals, and strong spin-orbit coupling (SOC) on Ir ions.

Low-energy properties of insulating iridates can be accurately described in terms of a pseudospin-1/2 magnetic model

$$\mathcal{H}_{ij} = J\,\tilde{\mathbf{S}}_i\cdot\tilde{\mathbf{S}}_j + \Gamma_\parallel \tilde{S}_i^x\tilde{S}_j^x + \Gamma_\perp \tilde{S}_i^y\tilde{S}_j^y + \Gamma^{zz}\tilde{S}_i^z\tilde{S}_j^z, \quad (3)$$

Without loss of generality the diagonal matrix Γ is taken to be traceless and then, for instance, $\Gamma^{zz} = -(\Gamma_\parallel + \Gamma_\perp)$. Four eigenstates of Eq.3 are the singlet $|\Psi_S\rangle = |\uparrow\downarrow - \downarrow\uparrow\rangle/\sqrt{2}$ and triplet states

$$|\Psi_1\rangle = |\uparrow\downarrow + \downarrow\uparrow)\rangle/\sqrt{2}, \qquad |\Psi_2\rangle = (\uparrow\uparrow + \downarrow\downarrow)/\rangle\sqrt{2},$$

and $|\Psi_3\rangle = (\uparrow\uparrow - \downarrow\downarrow)\rangle/\sqrt{2}$.

The corresponding eigenvalues are

$$E_S = -\frac{3}{4}J,$$
$$E_1 = \frac{1}{4}J + \frac{1}{2}\left(\Gamma_\parallel + \Gamma_\perp\right),$$
$$E_2 = \frac{1}{4}J - \frac{1}{2}\Gamma_\perp, \quad E_3 = \frac{1}{4}J - \frac{1}{2}\Gamma_\parallel. \quad (4)$$

Table 1: Energy splittings for the four lowest spin states of two NN IrO_6 octahedra and the calculated magnetic coupling constants (all in meV)

States/Method	CAS+SOC	MRCI+SOC
$\Psi_S(A_{1g}) = (\uparrow\downarrow - \downarrow\uparrow)/\sqrt{2}$	0.0	0.0
$\Psi_3(A_{1u}) = (\uparrow\uparrow - \downarrow\downarrow)/\sqrt{2}$	37.5	65.0
$\Psi_1(B_{2u}) = (\uparrow\downarrow + \downarrow\uparrow)/\sqrt{2}$	38.2	66.7
$\Psi_2(B_{1u}) = (\uparrow\uparrow + \downarrow\downarrow)/\sqrt{2}$	38.2	66.7
$(\bar{J},\bar{\Gamma}_\parallel)$	(36.8,0.75)	(65.02,3.4)

Of the 36 spin-orbit states that are obtained in QC calculations, the lowest four magnetic states which correspond to the low energy magnetic Hamiltonian in Eq. 3 are shown in Table 1 both at CASSCF (CAS+SOC) and MRCI (MRCI+SOC) levels.

The assignment of these states is made based on the nature of the dipole and quadrupole transition matrix elements, available in MOLPRO. The singlet Ψ_S for which $\tilde{\mathbf{S}}_{\rm tot} = \tilde{\mathbf{S}}_i + \tilde{\mathbf{S}}_j = 0$ is well below from the set of $\tilde{\mathbf{S}}_{\rm tot} = 1$ triplet states that are partially and weakly split thus indicating a large antiferromagnetic Heisenberg interaction J and a weak symmetric anisotropy $\sim \Gamma$. The QC calculations show that the triplet components Ψ_1 and Ψ_2 to be almost degenerate (differ by $0.1cm^{-1}$ in our results). With the neglect of this small difference, the QC calculations predicts an equality $\Gamma_\perp = \Gamma_{zz}$.

Now the Hamiltonian in Eq.3 can be rewritten as

$$\mathcal{H}_{ij} = \bar{J}\,\tilde{\mathbf{S}}_i\cdot\tilde{\mathbf{S}}_j + \bar{\Gamma}_\parallel\,\tilde{S}_i^\gamma\tilde{S}_j^\gamma, \qquad (5)$$

where $\bar{J} = J + \Gamma_\perp = 65.02$meV, $\bar{\Gamma}_\parallel = \Gamma_\parallel - \Gamma_\perp = 3.4$meV, and $\gamma = x(y)$ for a bond along $\mathbf{x}(\mathbf{y})$ axis in the basal-plane of Ba_2IrO_4.

Below $\sim$ 240K, Ba_2IrO_4 exhibits a basal-plane antiferromagnetic (AFM) order with collinear magnetic moments pointing along [1,1,0] direction. The compass-like magnetic model, Eq.5, on the square lattice of Ir ions is unable itself to predict the observed magnetic structure, and we have added delicate terms of weak interplane interactions, which selects the ground state suggested from experiment.

2D lattice model $\mathcal{H} = \sum_{<i,j>}\mathcal{H}_{ij}$ with couplings $\bar{J} \gg \bar{\Gamma}_\parallel > 0$ dictates an AFM ordering in the easy $xy-$plane. On the classical level, however, the model shows a continuous degeneracy with respect to rotation of the staggered magnetization moment in the plane. To check a type of the ground state structure selected with the "order by disorder" mechanism, we first assume that the AFM vector makes an angle ϕ with $\mathbf{x}$ axis, and define the zero-point quantum spin-wave energy (per spin) as fol-

lows

$$E_{ZP,2D}(\phi) = \frac{1}{2N}\sum_{\mathbf{q}} \left(\Omega_+(\mathbf{q}) + \Omega_-(\mathbf{q})\right). \qquad (6)$$

Here, $\Omega_\pm(\mathbf{q})$ are two branches of the spin-wave spectrum calculated with the model parameters $\bar{J}, \bar{\Gamma}_\parallel$ from Table 1, and the summation is over the Brillouin zone. Numerical analysis of Eq.6 shows that $E_{ZP,2D}(\phi)$ behaves as

$$E_{ZP,2D}(\phi) = -K\cos(4\phi) + E_0, \qquad (7)$$

with $K = 2\mu$eV and E_0 is a constant. Thus, for 2D lattice model the quantum fluctuations favor the AFM vector to point along a [1,0] direction within the easy plane.

Recalling now that in the similar situation occurring in several tetragonal planar cuprates with the same '214' lattice structure as in Ba_2IrO_4, the true ground state is provided by a special mechanism due to weak interplane interactions. Assuming that qualitatively the same 3D mechanism is applicable to Ba_2IrO_4 as well, we summarize below its main contributions to an expression for the 3D ground state energy and calculate a phase diagram, which may help one to select a unique ground state magnetic structure depending on parameters of interplane magnetic coupling in tetragonal '214' iridates.

First of all, the potentially dominant isotropic exchange $J_{\rm out}$ between magnetic moments in adjacent planes vanishes in the mean field sense because of the geometrical frustration in '214' structure, however, this interaction contributes to the zero-point energy. The angle ϕ defined above and indexed now with an integer n, $\phi \to \phi_n$, specifies a ground-state direction of the AFM vector lying in the $n-$th plane. Complementary to $\sum_n E_{ZP,2D}(\phi_n)$, the zero-point energy acquires the additional term describing correlations between adjacent planes

$$E_{ZP,3D} = -B\sum_n \cos(2\phi_n - 2\phi_{n+1}). \qquad (8)$$

Here, $B = C_3 J_{\rm out}^2/2\bar{J}$, C_3 is a small positive constant and, hence, $B > 0$ (and both signs of $J_{\rm out}$ are allowed). Eq.8 requires collinearity of the staggered magnetizations in the adjacent planes.

Next, the frustration effects in NN magnetic coupling of adjacent planes in the '214' structure are canceled when one includes the interplane symmetric anisotropy $\sim \Gamma_{\rm out}^{\alpha\beta}$. Since the midpoint of these out-of-plane bonds is the inversion center, the antisymmetric anisotropy is excluded, $\mathbf{D}_{\rm out} = 0$. With the use of symmetry arguments, we derived a contribution to the ground-state energy in the following form

$$E_{aniso,3D} = -A\sum_n \sin(\phi_n + \phi_{n+1}), \qquad (9)$$

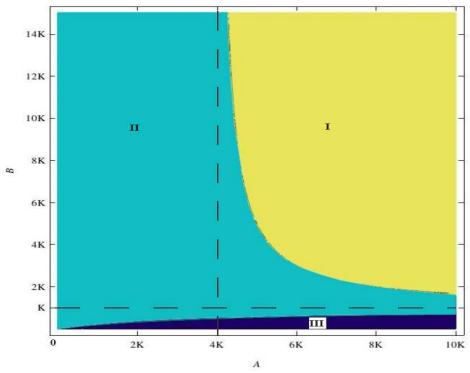

Figure 3: Phase diagram for Ba_2IrO_4.

where the constant A is determined by a relative strength of the symmetric anisotropy $\Gamma_{\rm out}$.

The total ground state energy now reads as $E = E_{ZP,2D} + E_{ZP,3D} + E_{aniso,3D}$ and is considered in the $A - B$ parameter space and fixed K. Minimization of E yields different 3D AFM structures denoted in the diagram, Fig.3, as phases I, II, and III. The main result of our subsequent analysis is the following. The collinear AFM structure experimentally observed in Ba_2IrO_4 can be naturally explained provided the parameters A and B in the ground-state energy fall into a broad region of the parameter space denoted as the phase I in the diagram presented in Fig.3.

To conclude, the suggested computational scheme of QC cluster calculations may be extended and applied to a description of selective RIXS transitions in other perovskites as well as to the study of magnetic properties of strongly correlated electron systems.

References

[1] L. Ament, M. van Veenendaal, T. P. Devereaux, J. P. Hill, and J. van den Brink, Rev. Mod. Phys. **83**, (2011) 705.

[2] V. Yushankhai, L. Siurakshina,*Analysis of crystal-field multiplets of V^{3+} ion in perovskite oxides for resonant inelastic X-ray scattering spectroscopy*, Int.J.Mod.Phys. B **27**, (2013) 1350185.

[3] L. Siurakshina, B. Paulus, V. Yushankhai, and E. Sivachenko, Eur. Phys. J. B **74**, 53 (2010)

[4] H.-J. Werner, P. J. Knowles, G. Knizia, F. R. Manby, M. Schutz et al., molpro 2010, *see* [http://www.molpro.net]

[5] V. M. Katukuri, V. Yushankhai, L.Siurakshina, J. van den Brink, and L. Hozoi, *Magnetic anisotropy and ground state structure in layered iridate Ba_2IrO_4*, subm. to Phys. Rev. B (2013).